Applied Surface Science 352 (2015) 28–32

Contents lists available at ScienceDirect

Applied Surface Science

journal homepage: www.elsevier.com/locate/apsusc

Optical and mechanical properties of nanocrystalline ZrC thin films grown by pulsed laser deposition

D. Craciun[a,*], G. Socol[a], E. Lambers[b], E.J. McCumiskey[c], C.R. Taylor[c], C. Martin[d], N. Argibay[e], D.B. Tanner[f], V. Craciun[a]

[a] Laser Department, National Institute for Laser, Plasma, and Radiation Physics, Magurele, Romania
[b] Major Analytical Instrumentation Center, College of Engineering, University of Florida, Gainesville, FL 32611, USA
[c] Mechanical and Aerospace Engineering, University of Florida, Gainesville, FL 32611, USA
[d] Ramapo College of New Jersey, USA
[e] Materials Science and Engineering Center, Sandia National Laboratories, Albuquerque, NM 87123, USA
[f] Physics Department, University of Florida, Gainesville, FL 32611, USA

ARTICLE INFO

Article history:
Received 18 November 2014
Received in revised form 8 January 2015
Accepted 10 January 2015
Available online 17 January 2015

Keywords:
ZrC
Hard coating
Pulsed laser deposition
Infrared optical properties

ABSTRACT

Thin ZrC films (<500 nm) were grown on (100) Si substrates at a substrate temperature of 500 °C by the pulsed laser deposition (PLD) technique using a KrF excimer laser under different CH_4 pressures. Glancing incidence X-ray diffraction showed that films were nanocrystalline, while X-ray reflectivity studies found out films were very dense and exhibited a smooth surface morphology. Optical spectroscopy data shows that the films have high reflectivity (>90%) in the infrared region, characteristic of metallic behavior. Nanoindentation results indicated that films deposited under lower CH_4 pressures exhibited slightly higher nanohardness and Young modulus values than films deposited under higher pressures. Tribological characterization revealed that these films exhibited relatively high wear resistance and steady-state friction coefficients on the order of $\mu = 0.4$.

1. Introduction

Zirconium carbide, ZrC, possesses both ceramic and metallic characteristics such as one of the highest melting point [1], very high hardness (30–35 GPa) [2,3], good wear resistance [4], and high thermochemical stability with a single fcc lattice from room temperature up to the melting temperature [5].

Several deposition techniques have been employed to obtain ZrC thin films to investigate their properties for various applications [3–8]. Pulsed laser deposition (PLD) is a very suitable technique for such studies, since by controlling laser irradiation parameters and deposition conditions films with various structural qualities can be obtained [3,9–11]. Moreover, crystalline films could be deposited at moderate substrate temperatures, below 550 °C. We showed previously that ZrC films grown by PLD at different temperatures exhibited high hardness and Young's modulus values, as well as low friction coefficients and wear rates [3,11]. We extended the investigations to elucidate the role of the deposition atmosphere on the optical and mechanical properties of ZrC thin films to optimize the properties and the results are presented below.

2. Experimental details

A KrF excimer laser ($\lambda = 248$ nm, pulse duration $\tau = 25$ ns, 8 J/cm^2 fluence, 40 Hz repetition rate) was used to ablate a ZrC target in a stainless steel chamber. The films were deposited for 20,000 pulses at a substrate temperature of 500 °C under different CH_4 pressures in order to study the effect of the deposition atmosphere on their structure and properties. The deposition conditions are displayed in Table 1.

The crystalline structure, grain size and micro-stress values were obtained from glancing incidence and symetrical X-ray diffraction (GIXD and XRD) investigations [11–13], while the mass density, thickness of the surface oxide-contamination layer, and surface roughness values (rms) were obtained from simulations of the XRR curves using a commercially available software (X'Pert Reflectivity). An atomic force microscope (AFM, Asylum Research MFP-3D) was also used to investigate the surface morphology of the deposited samples. Auger electron (AES, Perkin Elmer PHI 660) and X-ray photoelectron spectroscopy (XPS, PHI 5000

* Corresponding author.
E-mail address: doina.craciun@inflpr.ro (D. Craciun).

http://dx.doi.org/10.1016/j.apsusc.2015.01.076
0169-4332/

Table 1
Deposition conditions and structural properties of the deposited films.

Sample	Atmosphere [mbar]	Lattice parameter [Å]	Grain size [Å]	Micro-strain [%]
ZrC1	2×10^{-5} CH_4	4.735	108	0.82
ZrC2	2×10^{-4} CH_4	4.741	104	0.93
ZrC3	Vacuum	4.738	106	0.82

Table 2
XRR simulation and nanoindentation results (E and H, Young's modulus and nanohardness, respectively) for the deposited films.

Sample	Structure	Thickness [Å]	Density [g/cm^3]	Roughness [Å]		E[GPa]	H [GPa]
				XRR	AFM		
ZrC1	Contamination layer	22	4.52	13	6	247.6	40.2
	Deposited layer	NA	6.40				
ZrC2	Contamination layer	17	4.69	12	7	254.8	36.7
	Deposited layer	NA	6.36				
ZrC3	Contamination layer	17	4.98	14	6	259.7	40.0
	Deposited layer	NA	6.39				

Versaprobe II) were used to investigate the elemental composition of the deposited films.

The mechanical properties of the thin films were investigated using a Triboindenter (Hysitron, Minneapolis, MN) with a 100 nm diamond cube corner tip. To minimize substrate contributions, the hardness and reduced modulus were determined from load-displacement contact depths between 20 and 30 nm following the model of Oliver and Pharr [14]. In order to gain insight into the deformation mechanisms of the ZrC film, and its interaction with the interface between it and the underlying Si substrate, cross-sectional transmission electron microscopy (X-TEM) was employed to observe nanoindentation cross sections in the ~200 nm ZrC films on (100) Si. TEM imaging was performed using a 200CX TEM (JEOL, Tokyo, Japan) along the [100] zone axis, using a two-beam bright-field condition. Using the method described in detail in Ref. [15], a 13×4 array of 6-mN indents, spaced 2 μm apart, was made with a diamond cube-corner tip on an MPF-3D Nanoindenter (Asylum Research, Santa Barbara, CA). Using a Strata DB325 dual-beam focused ion beam (FIB)/SEM (FEI, Hillsboro, OR) to mill away a thin (~200 nm) cross section in the array of indents, with the slice offset by an optimum angle of ~6.6° [15], multiple, different sections of similar indents were guaranteed to be contained in a single X-TEM specimen. Room temperature optical reflectance was measured from 30 cm^{-1} (4 meV) to 30,000 cm^{-1} (4 eV), using a Bruker-113v FTIR spectrometer and a Carl Zeiss microscope photometer. Optical conductivity and dielectric constants were obtained from Kramers-Kronig transformation of reflectance data.

A linear reciprocating tribometer was used for friction and wear experiments, fully described in an earlier publication [16]. A normal force of 1 N ± 50 mN and sliding speed of 1 mm/s were used. The wear volume was measured using a scanning white light interferometer (SWLI; Veeco Wyko NT1100), and a multi-point measurement of wear rate computed to determine whether non-linear run-in behavior occurs. The length of the wear track was reduced progressively from 10 mm in 1 mm steps at intervals of 10, 100, 200 and 500 cycles, so that at the end of an experiment it was possible to determine the amount of wear at the end of each interval by analyzing the corresponding segments. Bearing grade silicon nitride (Si_3N_4) balls 1.59 mm in radius were used for the friction and wear experiments, and the contact spot changed for each experiment so as to use an untouched area of the ball.

3. Results and discussion

X-ray diffraction patterns acquired from the deposited ZrC films showed a slight (1 1 1) texture, usually observed for thin ZrC films that crystallize in the fcc lattice, where the (1 1 1) planes possess the highest atomic density [7,9]. Results of Williamson-Hall analysis, also displayed in Table 1, indicated that films were nanocrystalline and exhibited rather large microstress values.

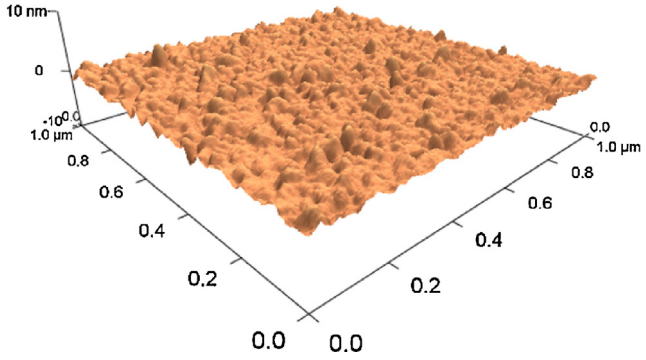

Fig. 1. AFM image of the ZrC3 sample's surface morphology.

The films' mass densities, thickness of the surface contamination layers and roughness values, obtained from simulations of the acquired XRR curves are displayed in Table 2. For simulations, a model consisting of two layers only was used (the deposited layer with infinite thickness and a surface contamination layer), since the thicknesses of the deposited films were larger than the X-ray penetration depth for the low incidence angles used during the measurements. The thickness of the top contamination layer was found to be around 20 Å and its density from 4.5 to 5.0 g/cm^3, indicative of an oxyhydride compound. One could note that the deposited films mass densities were very similar to bulk values [5,17] and the films' surfaces were very smooth. Very low rms surface roughness values were also confirmed by AFM images of the deposited films. Fig. 1 displays an image of the surface morphology acquired from ZrC3 sample. The rms values determined by AFM were usually slightly lower than those estimated from simulations of the XRR curves (see Table 2) since the investigated areas were different: 1 μm × 1 μm versus 10 mm × 0.1 mm for AFM and XRR, respectively, in agreement with other report [17].

AES survey spectra, as those shown in Fig. 2, recorded after removal of more than 10 nm of surface material by Ar ion sputtering, indicated low oxygen concentrations within the deposited films. The Zr to C ratios estimated from AES measurements were around 1.5, indicating either a strong preferential sputtering of the lighter C atoms or a substoichiometric compound, containing C vacancies. Since the Zr/C values seemed to be independent of the AES take-off angle, as it is apparent from inspecting the spectra displayed in Fig. 2, it could be safely inferred that the

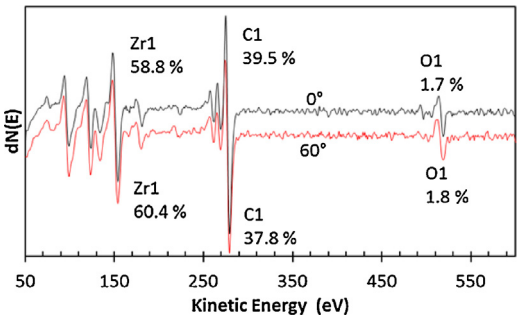

Fig. 2. AES survey spectra acquired at two different take off angles from sample ZrC3 after more than 10 min Ar ion sputtering.

deposited films contained a large concentration of C vacancies. Rutherford backscattering spectrometry investigations also supported this result, the measured Zr/C ratios agreeing quite well with the AES values. Representative XPS survey scan recorded from as deposited and Ar ion sputtered surfaces of the ZrC1 and ZrC3 films are displayed in Fig. 3. The oxygen concentration was quite low, confirming the AES results. The binding energy of the C 1s (281.6 eV) and Zr 3d (179.2 eV and 181.3 eV) peaks agreed very well with those reported for ZrC compounds [7,17,18].

Measured optical reflectance and the calculated optical conductivity are shown in Fig. 4. It can be seen that in the far-infrared (low frequency) region, reflectance exceeds 90% for all films, indicating metallic behavior. Also, in mid-infrared it can be observed a clear, slightly broadened, plasma edge, associated with plasma frequency of the free carriers. From the optical conductivity data it follows that the zero frequency (Drude) electrical conductivity is about 1300–900 Ω^{-1} cm^{-1}, hence the resistivity is 770–1100 μΩ cm. These value are higher than those reported for the bulk or thicker films of around 100–200 μΩ cm [5], possibly because of the relatively high scattering rate of the free carriers in these nanocrystalline films, which is also responsible for the broadening of the plasma edge in reflectance data, but quite in line with other reports for similar films [7]. The free carrier parameters (plasma frequency ω_p, scattering rate $1/\tau$ and Drude conductivity $\sigma(0)$), obtained from fits with a Lorentz–Drude model of both reflectance and optical conductivity, are shown in Table 3. Assuming the effective mass to be that of the free electron mass, the carrier concentration in our films would be ~10^{21} cm^{-3}, characteristic of metals. Fig. 5 shows the imaginary part of the dielectric constant (ε_2) for all films, plotted versus wavelength, in the visible and near infrared spectral region. The values are larger than those measured for Ag or Au, but very similar to those reported for TiN films, which were shown to be useful for plasmonics applications [19].

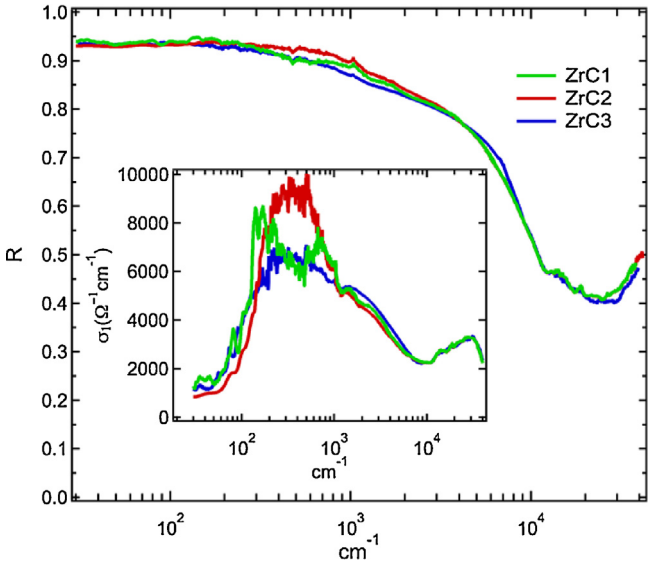

Fig. 4. Room temperature optical reflectance $R(\omega)$ (main panel) and optical conductivity $\sigma_1(\omega)$ (inset) of ZrC thin films.

Table 3
Electrical properties of the ZrC films calculated from the reflectance data.

	ω_p (eV)	$1/\tau$ (eV)	$\sigma(0)$ (Ω^{-1} cm^{-1})
ZrC1	1.4	0.4	1300
ZrC2	1.4	0.5	900
ZrC3	1.6	0.5	1000

Nanoindentation results, displayed in Table 2, indicated that films were quite hard, exhibiting values that were up to 40 GPa. Such large hardness values could be explained by a combination of very high density and nanometer size crystallites, containing a large concentration of defects that results in a large micro-stress value, as indicated by the XRD analysis. Dislocations could not easily form in such small crystallites or, if they form, the defects will impede their movement when pressure is applied.

Fig. 6 shows friction and wear data for two PLD grown ZrC films, in sliding against a silicon nitride spherical indenter, with a maximum Hertzian contact pressure of approximately 1.2 GPa, a value that is significantly lower than the hardness of the film and indenter materials [3,11] and so indicative of a wear regime that is conservatively below gross plastic deformation (macroscopic plowing). The films both exhibited an initial friction coefficient of $\mu = 0.2$ that increased to steady-state values between $\mu = 0.4$ to 0.5 over the first 20 cycles. A sharp increase in friction coefficient to $\mu = 0.6$

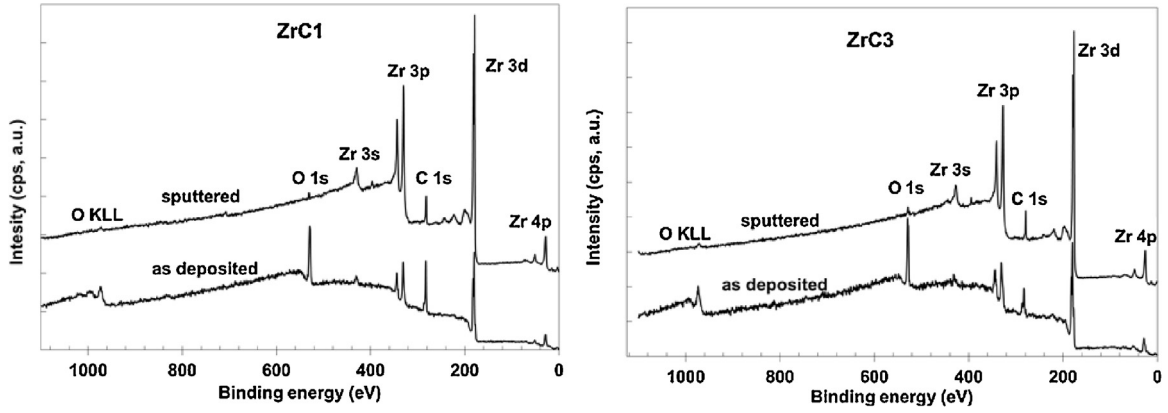

Fig. 3. XPS survey scan recorded from the as-deposited and bulk of ZrC1 and ZrC3 films.

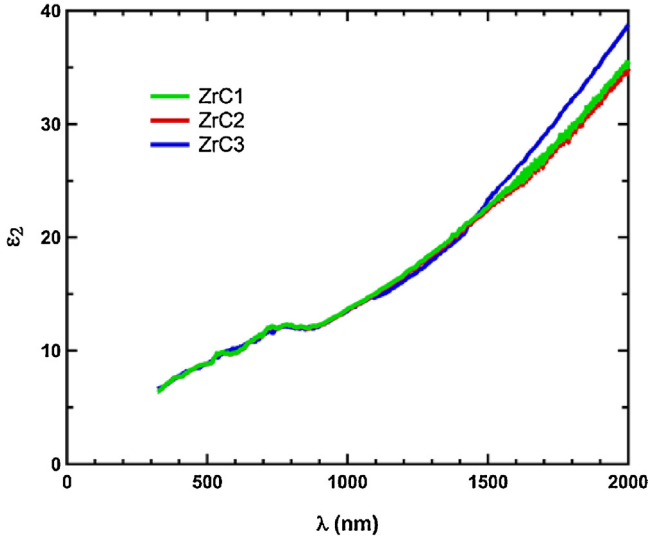

Fig. 5. Imaginary part of the dielectric constant ε_2 (vs. wavelength) of ZrC thin films.

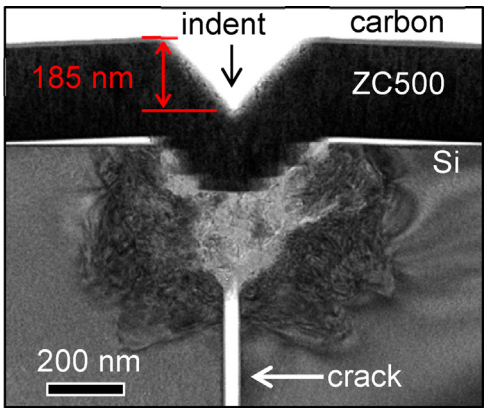

Fig. 7. X-TEM image of a nanoindentation site in a ZrC1 film on (1 0 0) Si.

observed after many cycles is associated with wear-through of the ZrC films and exposure of the underlying substrate. The steady-state friction behavior of these PLD grown ZrC films was slightly higher than the values measured for a PLD grown ZrN thin film [11]. The specific wear rate, K (mm^3/N m), was calculated based on the SWLI measurements only for the sliding intervals of wear track that correspond to film wear, where the underlying substrate was not exposed. The measured wear volumes of both films after 10 cycles of sliding were negligible and of the same order as the surface roughness of the film. While there is an evident transient in the friction behavior over the first 20 cycles, the wear data suggests that there was not a significant transient in wear rates. The transient in friction behavior is likely a result of the evolution in surface roughness from atomically smooth to a higher steady-state roughness. This behavior can be described analytically as a change in the plasticity index proposed by Greenwood and Williamson [20], implying that with increasing roughness the probability increases that micro-asperity contact events on the average generate localized stresses exceeding the yield of the materials. In other words, contact between these initially smooth surfaces is likely to be predominately elastic until the roughness increases sufficiently so that micro-asperity contact events transition on the average toward a higher probability for plastic behavior. Specific wear rates between $7.1–7.8 \times 10^{-5}$ mm^3/N m were found for ZrC films. Although these are quite low values, they were higher than the 4.5×10^{-6} mm^3/N m value measured for a high quality, very smooth ZrN film [11]. Nonetheless, the films were quite adherent to the Si substrate.

A cross-sectional TEM image of a nanoindentation site, performed with a very large load (6 mN), that resulted in an indentation depth of around 185 nm, is shown in Fig. 7. It was surprising to observe that the ZrC film did not fracture for such a high load indentation, which resulted in severe deformation of the film. A median crack in the (100) Si substrate can be observed beneath the nanoindentation site. Some lateral detachment of the deposited film from the Si substrate on a 200 nm lateral distance from the indentation site can also be observed, otherwise the films being very adherent to the substrate.

4. Conclusions

ZrC films were grown on Si substrates using the PLD technique at 500 °C. The CH_4 pressure used during deposition had a marginal effect on the structural properties (grain size and microstress values) and chemical composition. Optical reflectometry measurements showed that films exhibited metallic characteristics, with R values around 0.90 in the infrared range. From the optical conductivity data it followed that the zero frequency electrical conductivity reached the highest value of about 1300 Ω^{-1} cm^{-1} for the ZrC film deposited under 2×10^{-5} mbar of CH_4. Nanoindentation and wear tests also showed that these film exhibited slightly better mechanical properties than those deposited at higher CH_4 pressures.

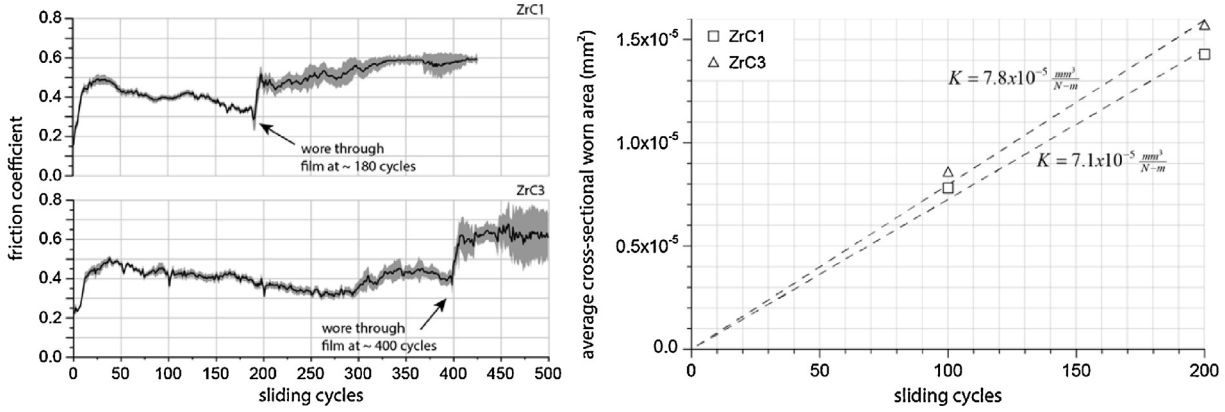

Fig. 6. Friction and wear data as a function of sliding cycles for ZrC1 and ZrC3 films.

Acknowledgement

This work was supported by grants of the Romanian Ministry of Education, ROSA STAR project number 60/2013 and CNCS–UEFISCDI project Ideas 337/2011. Part of this work was supported by Sandia National Laboratories, a multi-program laboratory managed and operated by Sandia Corporation, a wholly owned subsidiary of Lockheed Martin Corporation, for the U.S. Department of Energy's National Nuclear Security Administration under contract DE-AC04-94AL85000.

References

[1] L.E. Toth, Transition Metal Carbides, Academic, New York, 1971.
[2] W. Lengauer, Transition metal carbides, nitrides and carbonitrides, in: R. Riedel (Ed.), Handbook of Ceramic Hard Materials, vol. 1, Wiley-VCH, Weinheim, 2000.
[3] V. Craciun, E.J. McCumiskey, M. Hanna, C.R. Taylor, J. Eur. Ceram. Soc. 33 (2013) 2223–2226.
[4] D. Craciun, G. Socol, G. Dorcioman, S. Niculaie, G. Bourne, J. Zhang, E. Lambers, K. Siebein, V. Craciun, Appl. Phys. A 110 (2013) 717–722.
[5] Y. Katoh, G. Vasudevamurthy, T. Nozawa, L.I. Snead, J. Nucl. Mater. 441 (2013) 718–742.
[6] Y. Long, A. Javed, J. Chen, Z.K. Chen, X. Xiong, Ceram. Int. 40 (2014) 707–713.
[7] Q.N. Meng, M. Wen, F. Mao, N. Nedfors, U. Jansson, W.T. Zheng, Surf. Coat. Technol. 232 (2013) 876–883.
[8] C. Liu, B. Liu, Y. Shao, Z.Q. Li, C.H. Tang, J. Am. Ceram. Soc. 90 (2007) 3690–3693.
[9] D. Craciun, G. Socol, N. Stefan, I.N. Mihailescu, G. Bourne, V. Craciun, Surf. Coat. Technol. 203 (2009) 1055–1058.
[10] D. Craciun, G. Bourne, J. Zhang, K. Siebein, G. Socol, G. Dorcioman, V. Craciun, Surf. Coat. Technol. 205 (2011) 5493–5496.
[11] G. Dorcioman, G. Socol, D. Craciun, N. Argibay, E. Lambers, M. Hanna, C.R. Taylor, V. Craciun, Appl. Surf. Sci. 306 (2014) 33–36.
[12] D. Simeone, G. Baldinozzi, D. Gosset, G. Zalczer, J.F. Berar, J. Appl. Crystallography 44 (2011) 1205–1210.
[13] C.H. Ma, J.H. Huang, H. Chen, Thin Solid Films 418 (2002) 73–78.
[14] W.C. Oliver, G.M. Pharr, J. Mater. Res. 47 (1992) 1564.
[15] E.J. McCumiskey, N.G. Rudawski, W.G. Sawyer, C.R. Taylor, J. Mater. Res. 28, 2637–2643.
[16] N. Argibay, S.V. Prasad, R.S. Goeke, M.T. Dugger, J.R. Michael, Wear 302 (2013) 955–962.
[17] A. Singh, M.H. Modi, R. Dhawan, G.S. Lodha, AIP Conf. Proc. 1591 (2014) 869.
[18] D. Craciun, G. Socol, N. Stefan, G. Bourne, Appl. Surf. Sci. 255 (2009) 5260–5263.
[19] G.V. Naik, J.L. Schroeder, X. Ni, A.V. Kildishev, T.D. Sands, A. Boltasseva, Opt. Mater. Exp. 2 (2012) 478.
[20] J.A. Greenwood, J.B.P. Williamson, Proc. R. Soc. Lond. A Math. Phys. Sci. 295 (1996) 300–319.